MICROSTRUCTURAL AND MECHANICAL PERFORMANCE OF Al_2O_3 NANOPARTICLE REINFORCED 17-4 PH STAINLESS STEEL BULK COMPOSITE PARTS FABRICATED BY LASER ENGINEERED NET SHAPING PROCESS

Fuda Ning[a], Yingbin Hu[a], Zhichao Liu[a], Hui Wang[a], Weilong Cong[a]*, Yuzhou Li[a,b]

[a]Department of Industrial Engineering, Texas Tech University, Lubbock, Texas, 79409, USA
[b]School of Electromechanical Engineering, Guangdong University of Technology, Guangzhou, Guangdong, 510006, China.
*Corresponding author: weilong.cong@ttu.edu

Abstract

Alloy 17-4 PH (AISI 630) is a precipitation-hardening martensitic stainless steel that has been extensively employed in the industries of aerospace, marine, and chemical. In this study, bulk parts of both 17-4 PH and Al_2O_3 reinforced 17-4 PH composites were fabricated on a steel substrate by laser engineered net shaping (LENS) process to investigate the effects of Al_2O_3 reinforcements on the part performance. The 17-4 PH powders were pre-mixed with Al_2O_3 nanoparticles by ball milling. The microstructures of both parts were observed using scanning electron microscopy and mechanical properties including microhardness and compressive properties were evaluated by means of a Vickers microhardness tester and a universal tester, respectively. The results indicate that Al_2O_3 reinforced 17-4 PH composite parts fabricated by LENS process exhibited superior microhardness and compressive properties as compared to pure 17-4 PH parts.

Keywords

Laser engineered net shaping (LENS); Al_2O_3 nanoparticle reinforced composites; Microstructures; Microhardness; Compressive properties.

1 Introduction

Alloy 17-4 PH (AISI 630) is a precipitation-hardening martensitic stainless steel that has been widely utilized in extensive fields including aerospace, marine, chemical, and infrastructure. These applications are desiring to enhance the requirement for the parts with a combination of superior strength, high hardness, and excellent wear resistance [1]. However, pure stainless steel alloys hardly possess all the aforementioned mechanical properties and fail to meet the mechanical demands under severe conditions. In order to improve the performance of the steel components, fabricating the ceramic reinforced stainless steel matrix composites (SSMCs) is an effective method due to the mechanical properties improvement contributed by the ceramic material reinforcements.

Ceramic reinforced SSMC parts can be fabricated by conventional techniques including casting and powder metallurgy. However, these two conventional techniques exhibit difficulties in fabricating the composite parts with complex structures. In comparison to the conventional casting and powder metallurgy techniques, laser additive manufacturing (LAM) methods own

the advantages of freeform part fabrications, high manufacturing efficiency, and easy controllability [2-4]. As one of the promising LAM techniques, laser engineered net shaping (LENS) process provides an irreplaceable solution to fabricate ceramic reinforced SSMC parts due to its specific capabilities of part remanufacturing, small heat-affected zone, refined microstructures, etc. [5]. The schematic of LENS fabrication process is illustrated in Figure 1. The powders delivered by the flowing inert gas stream are melted by the laser radiation ejected from the laser source, forming a high-temperature molten pool on the substrate. The molten pool will continuously catch and melt more powders leading to an increase of the volume. After the leaving of laser beam radiation, the molten pool begins to solidify as a consequence of the heat dissipation. As the powder stream and laser beam move according to the trajectory of designed structures, the first layer is deposited on the substrate. Afterwards, the laser deposition head ascends one layer thickness to a new position for the next layer fabrication. Such process will be repeated many times until a designed three-dimensional (3D) structure is built layer by layer.

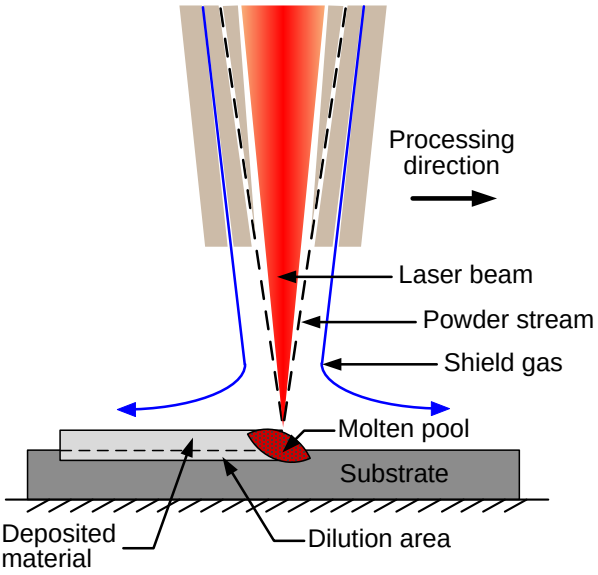

Figure 1. Laser engineered net shaping (LENS) process.

Due to the raw material availability, manufacturing costs, and excellent resistance to high temperature, wear, and corrosion, Al_2O_3 serves as one of the most widely applied ceramic reinforcements for SSMC part fabrications. Several investigations have been conducted on LENS manufacturing of Al_2O_3 reinforced SSMC coatings for surface modifications using the Al_2O_3 feedstock powders with an average particle size range of 40–100 μm [6-8]. The results indicated that the composite coatings possessed the enhanced microhardness, wear resistance, and corrosion resistance properties. However, Al_2O_3 (especially in nano size) reinforced SSMC parts fabricated by LENS process have not been reported in the open literature. Successfully fabricating Al_2O_3 nanoparticle reinforced SSMC parts using LENS will be beneficial for the production of key industrial components with remarkably improved mechanical properties.

In this paper, nanosized Al_2O_3 powders and 17-4 PH stainless steel alloy powders were pre-mixed by ball milling before LENS fabrication. Bulk pure stainless steel parts and SSMC parts were fabricated under two different laser powers using LENS process. Comparisons between the two types of parts were conducted to investigate the effects of Al_2O_3 nanoparticle reinforcements on the microstructures and mechanical properties.

2 Experimental set-up and measurement procedures

2.1 Materials

17-4 PH stainless steel alloy is defined due to its chemical composition of 17% chromium and 4% nickel. In this work, the as-received 17-4 PH stainless steel powders (Carpenter Powder Products Inc., Bridgeville, PA, USA) with a particle size range of 45–105 μm and 0.6 wt.% nanosized Al_2O_3 powders (Atlantic Equipment Engineers Inc., Upper Saddle River, NJ, USA) with a minimum particle size of 100 nm were pre-mixed using a planetary ball mill machine (ND2L, Torrey Hills Technologies LLC., San Diego, CA, USA). The morphology of SSMC powders after being ball milled for 3 hours are shown in Figure 2. It can be observed that the Al_2O_3 nanoparticles were uniformly distributed and attached on the surface of stainless steel powders.

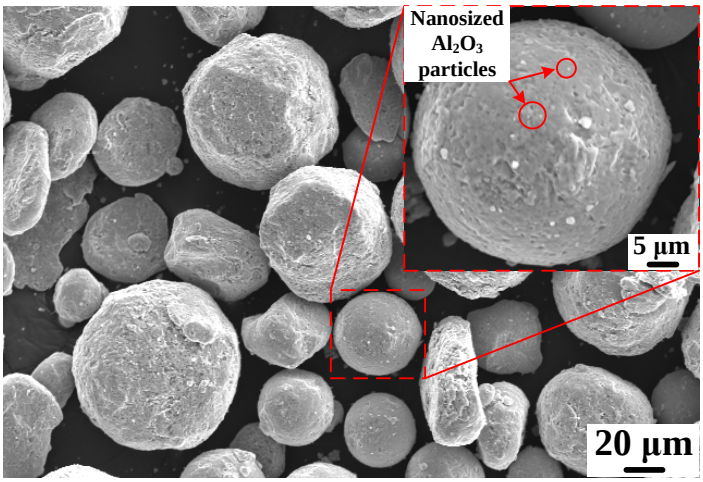

Figure 2. The morphology of Al_2O_3 nanoparticle reinforced SSMC powders

Low carbon steel plates (McMaster-Carr Co., Elmhurst, IL, USA) with dimensions of 100 mm × 50 mm × 6.4 mm were used as the substrate material. The plate surface was polished and then cleaned by acetone prior to the LENS fabrication.

2.2 Experimental conditions

The LENS process was conducted on a customized laser additive manufacturing system (450XL, Optomec Inc., Albuquerque, NM, USA). The experimental set-up mainly included an IPG fiber laser source with a maximum output power of 400 W, a coaxial deposition head for powder and inert gas delivery, and a 3-axes motion numeric control system. The bulk pure stainless steel parts and SSMC parts with square dimensions of 8 mm were built by LENS process. The specific LENS manufacturing parameters for bulk part fabrications were listed in Table 1.

Table 1. The LENS manufacturing parameters for bulk part fabrication.

Parameter	Value	Unit
Laser power	240, 300	W

Powder flow rate	3	g/min
Argon gas flow rate	6	L/min
Axis feedrate (contour)	635	mm/min
Axis feedrate (infill)	508	mm/min
Number of layers	2	
Increment of Z axis	0.38	mm
Hatch space	0.3	mm
Hatch angle (first layer)	45	°
Hatch angle interval	90	°

2.3 Characterizations of microstructures and mechanical properties

After LENS process, samples were prepared by standard metallographic techniques to observe and analyze the deposition defects and microstructures under a field emission scanning electron microscopy (FE-SEM) (S4300, Hitachi Co., Tokyo, Japan). The sectioned samples were ground and polished on a grinder-polisher machine (MetaServ 250, Buehler, Lake Bluff, IL, USA) and then etched in a 50% hydrochloric acid solution for 3 mins to reveal the cross-sectional microstructures of the parts.

Microhardness on the transverse surface of the polished bulk parts was measured using a Vickers microhardness tester (900–390A Phase II, Metal-Testers Inc., Nanuet, NY, USA). The test was performed at a normal load of 9.8 N and a dwelling time of 15 s. Ten random-position indentations were conducted on the transverse surface of each sample.

Table 2. The LENS manufacturing parameters for compressive cylinder fabrication.

Parameter	Value	Unit
Laser power	240, 300	W
Powder flow rate	2	g/min
Argon gas flow rate	6	L/min
Axis feedrate (contour)	635	mm/min
Axis feedrate (infill)	508	mm/min
Number of layers	8	
Increment of Z axis	0.43	mm
Hatch space	0.3	mm
Hatch angle (first layer)	60	°
Hatch angle interval	60	°

The compressive cylinders with a diameter of 3.5 mm were fabricated for the compressive test in this work. Three cylinders were prepared for each processing condition. The specific LENS manufacturing parameters for compressive cylinder fabrications were listed in Table 2. The top and bottom surfaces of each cylinder were ground by the grinder-polisher machine prior to the compressive test. Then the compressive tests were conducted using a universal testing machine (AGS-X, Shimadzu Co., Kyoto, Japan) with a 50 kN load cell capacity at a constant crosshead speed of 0.3 mm/min. The relationships between force (N) and displacement (mm) were collected by a computer with the help of a data acquisition software (Trapezium, Shimadzu

Co., Kyoto, Japan). The compressive properties including ultimate compressive strength, yield strength, and toughness would be obtained.

3 Results and discussion

3.1 Microstructures

The effects of Al_2O_3 reinforcements and laser powers on the porosity of the LENS-fabricated bulk parts can be seen in Figure 3. During LENS process, pores were always generated in the cross section area due to the evolution of entrapped gas bubbles in the molten pool. These pores were hardly expelled from the top surface prior to the metal solidification in LENS. In addition, cavities mainly occurred around the interface between the fabricated parts and substrate, which were generated due to the shrinking behavior of the localized molten pool and convection flow driven by the surface tension during the high-speed solidification process [9].

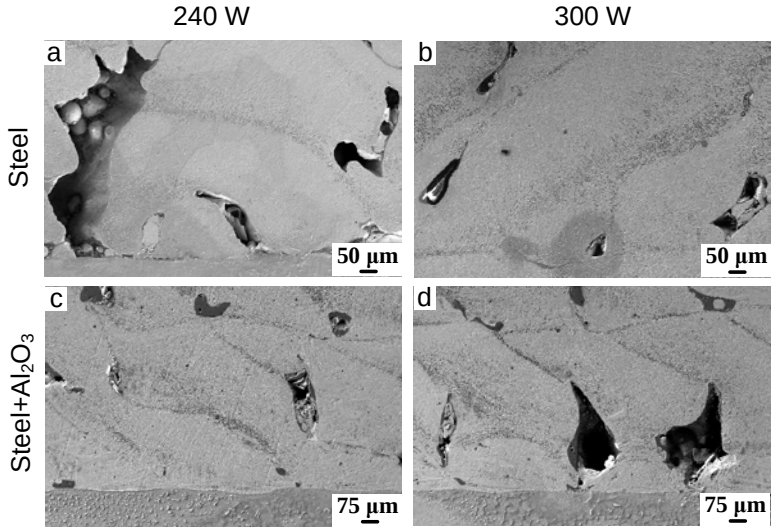

Figure 3. Pores and cavities evolution in the LENS-fabricated parts under two laser powers.

It can be seen from Figure 3a that large pores and cavities were caused in the pure stainless steel parts at the laser power of 240 W. Not fully melted steel powders could be also observed inside the cavities as a result of the insufficient laser energy. The increase of laser power to 300 W decreased the porosity and cavity to a certain level, as shown in Figure 3b. The possible reason is that the previous solidified tracks and layers could be remelted resulting in a better interfacial bonding between neighboring layers with less pores. With the adding of Al_2O_3 nanoparticle reinforcements into the SSMC parts, remarkably fewer pores and cavities were observed when the laser power was 240 W, as illustrated in Figure 3c. This is due to the fact that Al_2O_3 ceramic had a lower feasible region of laser power than stainless steel, thereby resulting in a better melting of the Al_2O_3 nanoparticle reinforced SSMC powders at the laser power of 240 W. The Al_2O_3 nanoparticles attached on the steel powers could be considered as the “catalyst” for the steel powder bonding. However, when laser power of 300 W was employed to fabricate Al_2O_3 reinforced SSMC parts, severe cavity was generated due to the relatively high laser energy that made Al_2O_3 nanoparticles evaporated from the matrix. The formation of pores and cavities

would lead to a weak bonding behavior between the fabricated parts and the substrate, and also weaken the mechanical properties of the fabricated parts.

3.2 Microhardness

A boxplot was used to represent the data distribution of microhardness values and the comparisons among different fabrication conditions were conducted using the boxplot, as shown in Figure 4. The boxplot was represented by mean, median, 25% and 75% percentile of confidence intervals, and outliers. It is notable that adding Al_2O_3 into the stainless steel matrix led to a significant increase of microhardness mean values using both laser powers. Especially at the lower laser power level of 240 W, microhardness mean values increased by 23% from 176 to 216 HV_1, which was larger than the enhancement obtained at the higher level of 300 W. In addition, for the pure stainless steel parts, the increase of laser power from 240 to 300 W contributed to an increase of microhardness mean values up to almost 190 HV_1. However, for the Al_2O_3 reinforced SSMC parts, the higher laser power level of 300 W was detrimental to the microhardness value that decreased from 216 to 200 HV_1. The possible reasons for these phenomena were that apart from the superior hardness of the rigid Al_2O_3 nanoparticle reinforcements, the decreased pores and cavities occurred in the Al_2O_3 reinforced SSMC parts was beneficial for the microhardness improvement compared with that in the pure stainless steel parts. Therefore, Al_2O_3 reinforcements contributed to the microhardness enhancement, though the evaporation of Al_2O_3 nanoparticles impaired the improvement of microhardness at the laser power of 300 W.

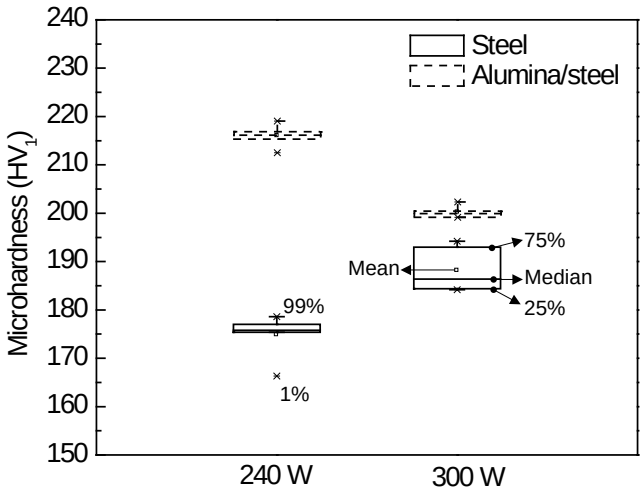

Figure 4. The effects of Al_2O_3 reinforcement and laser power on the microhardness

3.3 Compressive properties

The compressive test was conducted to evaluate the effects of Al_2O_3 reinforcement and laser power on the compressive properties including ultimate compressive strength (UCS), yield strength, and toughness. The compressive test would be terminated when the ductility (maximum strain) of the cylinder samples reached 50%. In this investigation, all the samples did not fracture within the 50% ductility limit during the test. The comparisons of each compressive property among different fabrication conditions were shown in Figure 5. The mean value was used to represent the trends of each property along with the increase of laser power. The error bar was represented by the standard deviation of the measuring data. It can be seen that all the compressive properties were significantly improved with the adding of Al_2O_3 nanoparticles into

the matrix due to the excellent performance of Al_2O_3 nanoparticles. In addition, Al_2O_3 reinforced SSMC parts exhibited a larger improvement of the properties at the laser power of 240 W in comparison to that at the laser power of 300 W. With the increase of laser power from 240 to 300 W, all the compressive properties exhibited an increase trend in the pure stainless steel parts and a decrease trend in the Al_2O_3 reinforced SSMC parts. Such phenomena were mainly ascribed to the decreased pores and cavities in the pure steel parts and the evaporation of Al_2O_3 nanoparticles at higher laser energy in the SSMC parts, respectively.

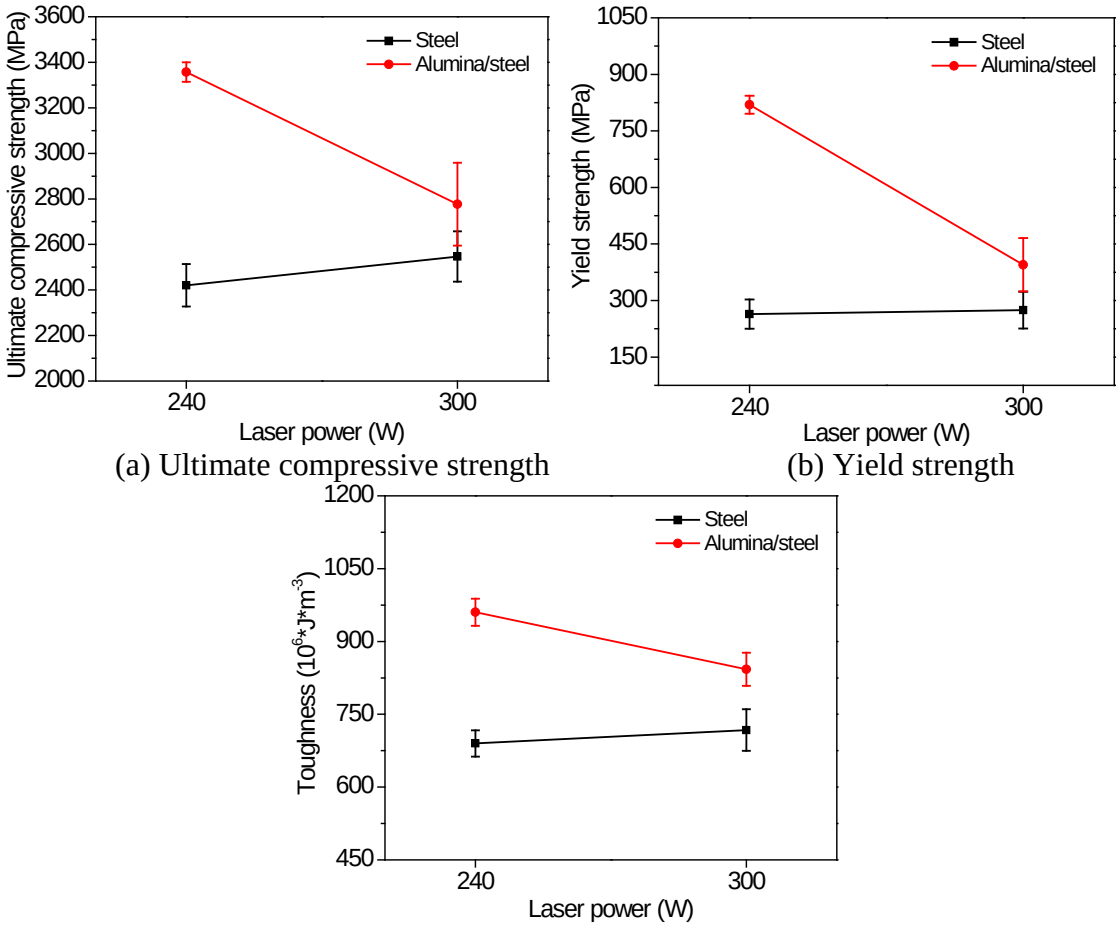

(a) Ultimate compressive strength (b) Yield strength

(c) Toughness

Figure 5. The effects of Al_2O_3 reinforcement and laser power on the compressive properties.

4 Conclusions

In this investigation, bulk stainless steel parts and Al_2O_3 nanoparticle reinforced SSMC parts were fabricated using LENS process. The effects of Al_2O_3 reinforcement and laser power on the microstructures and mechanical properties were evaluated. The main conclusions are drawn as follows:

(1) Pores and cavities were significantly reduced inside the Al_2O_3 nanoparticle reinforced SSMC parts at the laser power of 240 W. This is due to the fact that Al_2O_3 ceramic had a lower feasible region of laser power than stainless steel, thereby resulting in a better melting of the composite powders.

(2) Due to the strengthening effects of rigid Al_2O_3 nanoparticles, microhardness and compressive properties were improved in the Al_2O_3 nanoparticle reinforced SSMC parts compared with those in the pure stainless steel parts.

References

[1] Wang, H.M., Yu, Y.L., and Li, S.Q., 2002, "Microstructure and tribological properties of laser clad CaF_2/Al_2O_3 self-lubrication wear-resistant ceramic matrix composite coatings", Scripta Materialia, 47(1), 57-61.

[2] Frazier, W.E., 2014, "Metal additive manufacturing: a review", Journal of Materials Engineering and Performance, 23(6), 1917–1928.

[3] Thompson, S.M., Bian, L., Shamsaei, N., and Yadollahi, A., 2015, "An overview of direct laser deposition for additive manufacturing; Part I: Transport phenomena, modeling and diagnostics", Additive Manufacturing, 8, 36–62.

[4] Das, S., Beaman, J.J., Wohlert, M., and Bourell, D.L., 1998, "Direct laser freeform fabrication of high performance metal components", Rapid Prototyping Journal, 4(3), 112–117.

[5] Gu, D.D., Meiners, W., Wissenbach, K., and Poprawe, R., 2012, "Laser additive manufacturing of metallic components: materials, processes and mechanisms", International Materials Reviews, 57(3), 133-164.

[6] Duan, X.X., Gao, S.Y., Dong, Q., Zhou, Y.F., Xi, M.Z., Xian, X.P., and Wang, B., 2016, "Reinforcement mechanism and wear resistance of Al_2O_3/Fe-Cr-Mo steel composite coating produced by laser cladding", Surface and Coatings Technology, 291, 230-238.

[7] Xu, P., Lin, C.X., Zhou, C.Y., and Yi, X.P., 2014, "Wear and corrosion resistance of laser cladding AISI 304 stainless steel/Al_2O_3 composite coatings", Surface and Coatings Technology, 238, 9-14.

[8] Tan, H., Luo, Z., Li, Y., Yan, F., Duan, R. and Huang, Y., 2015, "Effect of strengthening particles on the dry sliding wear behavior of Al_2O_3–M_7C_3/Fe metal matrix composite coatings produced by laser cladding", Wear, 324, 36-44.

[9] Chen, S.L., and Hsu, L.L., 1998, "In-process vibration-assisted high power Nd:YAG pulsed laser ceramic–metal composite cladding on Al-alloys", Optics & Laser Technology, 30(5), 263–273.